

Vortex backwash during spatial evolution of “vortex” laser beams

V.P. Aksenov and A.V. Ustinov

*Institute of Atmospheric Optics,
Siberian Branch of the Russian Academy of Sciences, Tomsk*

Received March 24, 2003

A singular wave field was shown to have memory of optical vortices that existed in this field. After vortex annihilation, characteristic marks remain in the cross phase distribution. The phase near these marks exceeds essentially the phase in the adjacent area. Besides, vortex backwash manifests itself on the wave-front surface, where the vortex trail holds after vortex annihilation, and such wave front characteristics as the mean and Gaussian wave front curvatures are singular functions within the vortex trail. Some issues concerning the calculation of the phase distributing for singular wave fields are discussed.

Introduction

Vortex structures in the wave fields of any origin attract an increasing interest of investigators dealing with the wave propagation through linear and nonlinear media, as well as with the diagnostics of such media. Such structures are now studied most intensely in optics, where they are called optical vortices.^{1,2,3} An optical vortex is a local distribution of the field in the plane normal to the direction of wave propagation. The field strength at the vortex center is zero, and there is a field phase increment of $2\pi m$ along a closed contour that goes around the center (here m is an integer called the topological charge of the vortex). The wave front surface in the zone of an optical vortex is a spiral structure similar to that arising in the zone of a crystal lattice defect. It is for these reasons that such wave front singularities are called dislocations. As the radiation propagates through the medium, optical vortices arise, move, and annihilate.

On the one hand, this phenomenon hampers functioning of adaptive optics systems in the turbulent atmosphere,⁴ but, on the other hand, it favors a number of new applications thanks to many its marvelous properties. An optical vortex has the orbital angular momentum $m\hbar$ per photon,⁵ and this is a prerequisite for using vortices for optical manipulation of microscopic particles.

As known,^{1,2} vortices arising and annihilating in the process of laser beam propagation through a homogeneous or inhomogeneous medium do this by pairs, if only they did not already exist on the boundary of this medium. It is assumed that the wave front singularities annihilate simultaneously with the annihilation of vortices, and thus the wave front becomes smooth.⁶

However, it should be noted that in studying singular optical fields the attention is usually paid to the main value of the phase or the main value of the argument of the complex amplitude being a solution

to the wave equation. Nevertheless, there is a method for phase calculation based on integration of the phase gradient along the ray trajectories (lines of energy flow). This method is usually used in solving wave problems in the geometric optics approximation,⁷ but it can also be applied to calculation of the phase distribution, when diffraction phenomena should be taken into account. In this case, we should use the lines of energy flow calculated for the diffraction field (diffraction rays).^{8,9}

As known, the lines of the energy flow (diffraction rays) of a light beam in the vicinity of optical vortices look like spirals,¹⁰ therefore the ray length increases, as well as the phase change calculated along the rays. After the vortex annihilate, the rays are no longer spirals, but the phase increment caused by the spiral part keeps on. As a result, vortex backwash should be observed in the field of a light beam after vortex annihilation.

The aim of this paper is to study the spatial distribution of the phase (wave front) of an optical beam after annihilation of optical vortices with the topological charge of the opposite sign. The paper consists of three parts. The first part is a methodical one. Here we derive equations for phase calculation by the ray trajectories and consider limitations and special features associated with their application in the case of a diffraction singular wave field, as well as the use of a parabolic wave equation. The second part presents the model of the simplest singular wave field, which lies in the foundation of further calculations. The third part considers regularities of the wave front evolution for a singular beam at the stage following the vortex annihilation. The possibility of wave front approximation by a smooth surface is discussed as well.

1. Basic equations

The propagation of a harmonic light wave $U(\omega, \mathbf{p}, z) \exp \{i\omega t\}$ with the frequency ω through a homogeneous medium will be described using the

spectral amplitude $U(\omega, \mathbf{p}, z)$. Let us present it through real functions: amplitude $A(\omega, \mathbf{p}, z)$ and phase $S(\omega, \mathbf{p}, z)$:

$$U(\omega, \mathbf{p}, z) = A(\omega, \mathbf{p}, z) \exp \{iS(\omega, \mathbf{p}, z)\}, \quad (1)$$

where $\mathbf{p} = \{x, y\}$ is a two-dimensional vector. The spectral amplitude of the field $U(\omega, \mathbf{p}, z)$ obeys the Helmholtz equation

$$\Delta U(\omega, \mathbf{p}, z) + k_0^2 U(\omega, \mathbf{p}, z) = 0, \quad k_0 = \omega/c, \quad (2)$$

where c is the speed of light, $\Delta = \nabla \nabla$; $\nabla = \nabla_{\perp} + \mathbf{n} \frac{\partial}{\partial z}$,

$$\nabla_{\perp} = \mathbf{l} \frac{\partial}{\partial x} + \mathbf{m} \frac{\partial}{\partial y}.$$

Omitting, for brevity, the argument ω in the above complex and real functions, write¹¹ the system of equations equivalent to Eq. (2), but including the eikonal equations

$$\{\nabla S(\mathbf{p}, z)\}^2 = k_0^2 + \Delta A(\mathbf{p}, z)/[A(\mathbf{p}, z)] \quad (3)$$

and the transfer equations

$$\nabla \{A^2(\mathbf{p}, z) \nabla S(\mathbf{p}, z)\} = 0. \quad (4)$$

Equation (4) can be written as follows:

$$\text{div } \mathbf{L}(\mathbf{p}, z) = 0, \quad (5)$$

where $\mathbf{L}\{L_{\perp}, L_z\}$ is the energy flow density vector (Pointing vector) with the components

$$L_z = A^2(\mathbf{p}, z) \frac{\partial}{\partial z} S(\mathbf{p}, z), \quad L_{\perp} = A^2(\mathbf{p}, z) \nabla_{\perp} S(\mathbf{p}, z). \quad (6)$$

The set of flow lines, along which the light energy propagates, gives the illustrative idea of the spatial distribution of the power flux. The flow lines are integral curves of the first-order differential equation

$$\frac{dx}{dz} = \frac{L_x}{L_z}, \quad \frac{dy}{dz} = \frac{L_y}{L_z}. \quad (7)$$

Considering z as an independent variable, we can write Eq. (7) as

$$\frac{d\mathbf{p}(z)}{dz} = \frac{\mathbf{L}_{\perp}}{L_z}. \quad (8)$$

For particular values of z the structure of phase space can be studied by specifying the field of directions

$$\frac{dy}{dx} = \frac{L_y}{L_x}. \quad (9)$$

It follows from Eqs. (7) and definitions (6) that the energy flow lines coincide with the flow lines of the phase gradient. In other words, the direction of the Pointing vector coincides with the phase gradient, and all the flow lines of the phase gradient turn out to be the energy flow lines. The components of the phase gradient, in their turn, are components of the local wave vector

$$k\{k_x = \frac{\partial}{\partial x} S, \quad k_y = \frac{\partial}{\partial y} S, \quad k_z = \frac{\partial}{\partial z} S\}.$$

The energy flow lines are determined almost everywhere in space except for singular points (lines), at which the light flux density (6) vanishes. Such points are the points of zero amplitude (intensity) of the field (dislocations) and saddle points of the phase surface, at which the phase gradient components vanish. The phase at the zero lines of the field is uncertain. At these lines, the phase potentiality is disturbed, and the areas of "defect" (singular) phase can be considered as vortical threads similarly to the areas of concentrated vorticity in the dynamics of an ideal fluid.^{12,13} For such vector fields, the field potential defined as

$$S(x, y, z) = S(x_0, y_0, z_0) + \int_{\Gamma} \nabla S(x', y', z') \mathbf{dr}', \quad (10)$$

through its initial value $S(x_0, y_0, z_0)$ and the curvilinear integral (circulation) along an arbitrary curve Γ connecting, without self-intersections, the starting $\mathbf{r}_0\{x_0, y_0, z_0\}$ and final $\mathbf{r}\{x, y, z\}$ points, is known to be generally a multiple-valued function. Its values depend, in the general case, on the shape of a curve, along which the integral is taken. Let us take the energy flow lines as such curves. Since only one flow line passes through every spatial point (no line passes through the zero points), each of these lines is unambiguously determined by the position of its starting point. Thus, calculating integral (10) along the flow lines and having known the initial phase value, we can assign a sole phase value at any point along the flow line. Since on the flow line the phase gradient vector and the unit vector tangent to the curve Γ have the same direction, Eq. (10) can be written as

$$S(\mathbf{r}) = S(\mathbf{r}_0) + \int_{\Gamma} |\nabla S(\mathbf{r}')| \mathbf{dr}'. \quad (11)$$

And with the coordinate z used as an independent variable and taking into account that the length of an arc element is $dr = \sqrt{dx^2 + dy^2 + dz^2}$, Eq. (11) can be transformed to the form

$$S(\mathbf{p}, z) = S(z_0) + \int_{z_0}^z \sqrt{k_x^2[x(z'), y(z'), z'] + k_y^2[x(z'), y(z'), z'] + k_z^2[x(z'), y(z'), z']} \times \sqrt{1 + \left[\frac{d\mathbf{p}(z')}{dz'}\right]^2} dz'. \quad (12)$$

Eikonal equation (3) can be considered as the equation of the surface of wave vectors,¹¹ which is a sphere at any spatial point

$$k_x^2 + k_y^2 + k_z^2 = k_0^2 + \Delta A(\mathbf{p}, z)/[A(\mathbf{p}, z)]. \quad (13)$$

Only in the case of a plane wave this sphere has a constant radius k_0 . For an arbitrary field its value varies from point to point. Therefore, for determination of the wave vector component k_z from the two other

components as in many problems concerning wave propagation, in the case of an arbitrary wave field one should use equality (13), rather than the condition $k_x^2 + k_y^2 + k_z^2 = k_0^2$, which is valid only for plane waves.

Let the considered wave field be so that if the phase is represented in the form

$$S(\mathbf{p}, z) = k_0 z + S'(\mathbf{p}, z) \tag{14}$$

and, correspondingly, its derivative is

$$\frac{\partial}{\partial z} S(\mathbf{p}, z) = k_0 + \frac{\partial}{\partial z} S'(\mathbf{p}, z), \tag{15}$$

then the following inequality is fulfilled

$$\left| \frac{\partial S'}{\partial z} \right| \ll k_0, \tag{16}$$

which means that the phase S' varies only slightly at the wavelength. If, in addition, we can neglect diffraction in the longitudinal direction, assuming that the following inequality is valid:

$$\left| \frac{\partial^2}{\partial z^2} A(\mathbf{p}, z) \right| / [A(\mathbf{p}, z)] \ll k_0^2,$$

then the wave propagation can be considered in the approximation of the parabolic equation

$$2ik \frac{\partial V}{\partial z} + \Delta_{\perp} V = 0, \tag{17}$$

where

$$V(\mathbf{p}, z) = U(\mathbf{p}, z) \exp \{-ik_0 z\}.$$

Within the framework of this approximation, the eikonal and transfer equations have the form

$$2k_0 \frac{\partial S'}{\partial z} + \{\nabla_{\perp} S'\}^2 = \frac{\Delta_{\perp} A(\mathbf{p}, z)}{A(\mathbf{p}, z)}; \tag{18}$$

$$\nabla_{\perp} \{A^2(\mathbf{p}, z) \nabla_{\perp} S'\} = -k_0 \frac{\partial A^2}{\partial z}. \tag{19}$$

Fulfillment of equalities (14) and (15) means that the wave vector k can be represented in the form $k = k_0 \mathbf{n} + \mathbf{q}$, where $\mathbf{q} \{q_x = \frac{\partial}{\partial x} S', q_y = \frac{\partial}{\partial y} S', q_z = \frac{\partial}{\partial z} S'\}$.

In the quasioptical approximation,¹⁴ the surface of the wave vectors is approximated by a paraboloid

$$2k_0 q_z + q_x^2 + q_y^2 = \Delta_{\perp} A(\mathbf{p}, z) / [A(\mathbf{p}, z)], \tag{20}$$

and Eq. (12) is transformed into the following equality:

$$S(\mathbf{p}, z) = S(z_0) + \int_{z_0}^z \sqrt{[k_0^2 + q_x^2(z') + q_y^2(z')]} \times \\ \times \sqrt{\left\{ 1 + \left[\frac{d\mathbf{p}'(z')}{dz'} \right]^2 \right\}} dz', \tag{21}$$

where

$$\frac{d\mathbf{p}'(z')}{dz'} = \frac{\nabla_{\perp} S'}{k_0} = \frac{\mathbf{q}_{\perp}}{k_0}. \tag{22}$$

For the plane waves it was found¹⁴ that the spherical surfaces of the wave vectors are well approximated by paraboloids, if, in addition to condition (16) ($|q_z|/k_0 \ll 1$), the condition of small angles

$$|\mathbf{q}_{\perp}|/k_0 < 1 \tag{23}$$

or the condition of a pencil beam is fulfilled as well. Let us show that for the wave field in the vicinity of an optical vortex the latter is not fulfilled. For this purpose, select the solution of Eq. (17) in the form $V(\mathbf{p}, z) = x + iy$, wherefrom we have $A(\mathbf{p}, z) = \sqrt{(x^2 + y^2)}$. Then Eq. (20) for the surface of wave vectors degenerates into the equation of a circular cylinder

$$q_x^2 + q_y^2 = \frac{1}{(x^2 + y^2)}, \tag{24}$$

whose radius (and the value of the local cross wave vector) increases unlimitedly as the observation point approaches the center of the optical vortex. This means that the energy flow near the vortex axis is directed at a large angle to the beam axis. In this connection there is a risk of concepts substitution. Thus, if we assume that a pencil beam is a beam, in which the energy propagates only at small angles to the axis, then our singular beam cannot be considered as a pencil beam. Therefore, there are some doubts in the correctness of description of singular wave fields by the parabolic equation, because it is commonly known that the parabolic equation works well only for pencil beams. These doubts can be dispelled if we consider resolution of our elementary singular field in the spectrum of plane waves. Actually, requirement (23) is formulated only for plane waves. For the $v(\mathbf{\kappa}_{\perp})$ -dimensional spectrum of the "slow" function $x + iy$ we have

$$v(\mathbf{\kappa}_{\perp}) = \frac{1}{4\pi^2} \int_{-\infty}^{\infty} (x + iy) \exp(-i\mathbf{\kappa}_{\perp} \mathbf{\rho}) d^2 \rho = \\ = -\delta(\kappa_x) \delta'(\kappa_y) + i\delta'(\kappa_x) \delta(\kappa_y),$$

where $\mathbf{\kappa}_{\perp} = \{\kappa_x, \kappa_y\}$, $\delta(\mathbf{\kappa})$ and $\delta'(\mathbf{\kappa})$ are the Dirac delta function and its derivative, respectively. The equality obtained means that the spectral resolution of our function is nonzero only on the axis z , that is, our singular beam is a pencil beam.¹⁴ Thus, the unlimited increase of the cross components of the phase gradient (components of the cross wave vector) is not a signal of the need in some limitations in the application of the parabolic equation just near the center of the optical vortex. Such a limitation can be accepted only to simplify Eq. (21), which takes the following form if Eq. (22) is fulfilled

$$S(\mathbf{p}, z) = S(z_0) + \\ + k_0 \int_{z_0}^z \left\{ 1 + \frac{1}{2} \left[\frac{d\mathbf{p}'(z')}{dz'} \right]^2 \right\} dz'. \tag{25}$$

2. Model of the field with optical vortices

As an object for study, let us take the Laguerre–Gauss beam with a complex field amplitude of the form

$$V(x, y, z) = \frac{\Omega}{(1 + \Omega^2)^3} \exp \left\{ -\frac{\Omega^2 (x^2 + y^2)}{2a^2 (1 + \Omega^2)} + i \frac{\Omega (x^2 + y^2)}{2a^2 (1 + \Omega^2)} \right\} (V_r + iV_i)(1 + i\Omega)^3, \quad (26)$$

where

$$V_r = -3 + 2\Omega - \Omega^2 + 2 \frac{\Omega^2}{a^2} (x^2 + y^2 - xy),$$

$$V_i = 3 + 2\Omega + \Omega^2 - 2 \frac{\Omega^2}{a^2} (x^2 + y^2 + xy),$$

$\Omega = k_0 a^2 / z$ is the generalized diffraction parameter; a is the beam radius. Let $\lambda = 0.63 \mu\text{m}$, $a = 0.05 \text{ m}$. As was shown in Ref. 10, dislocations in the laser beam with such parameters exist already at the output from the laser ($z = 0$), then they annihilate at the diffraction parameter $\Omega = 3$ and revive at $\Omega = 1$. The stages of transformation of the singular field (26) have been thoroughly described in Ref. 10; therefore, in this paper we consider the formation of the wave front of a laser beam after annihilation of dislocations.

3. Lines of energy flow and formation of wave front of laser beam after annihilation of optical vortices

Let us first present the distribution of the intensity $I(\mathbf{p}, z) = A^2$ and the main (in the interval $[-\pi, \pi]$) phase values at the laser beam entrance $\Omega = 5.0$ ($z_0 = 5 \cdot 10^3$) and in the plane z_1 corresponding to the diffraction parameter $\Omega = 2.5$ ($z_1 = 10^4$) as calculated by Eqs. (26). These data are given in the first and second columns in Fig. 1. The third column depicts the directions of ray propagation in the cross plane xOy with the given value of the longitudinal coordinate z (the field of directions of the Pointing vector or the phase gradient) as calculated by Eq. (9). Recall¹⁰ that dislocations annihilate through bifurcation of singular points: a pair of unsteady focuses (Fig. 1a) – a pair of steady–unsteady node (Fig. 1b).

The phase distribution shown in Fig. 1 was calculated from the complex amplitude of the field (26) as the main value of the argument of this function

$$\tilde{s}(\mathbf{p}, z) = \arg [V(\mathbf{p}, z)]. \quad (27)$$

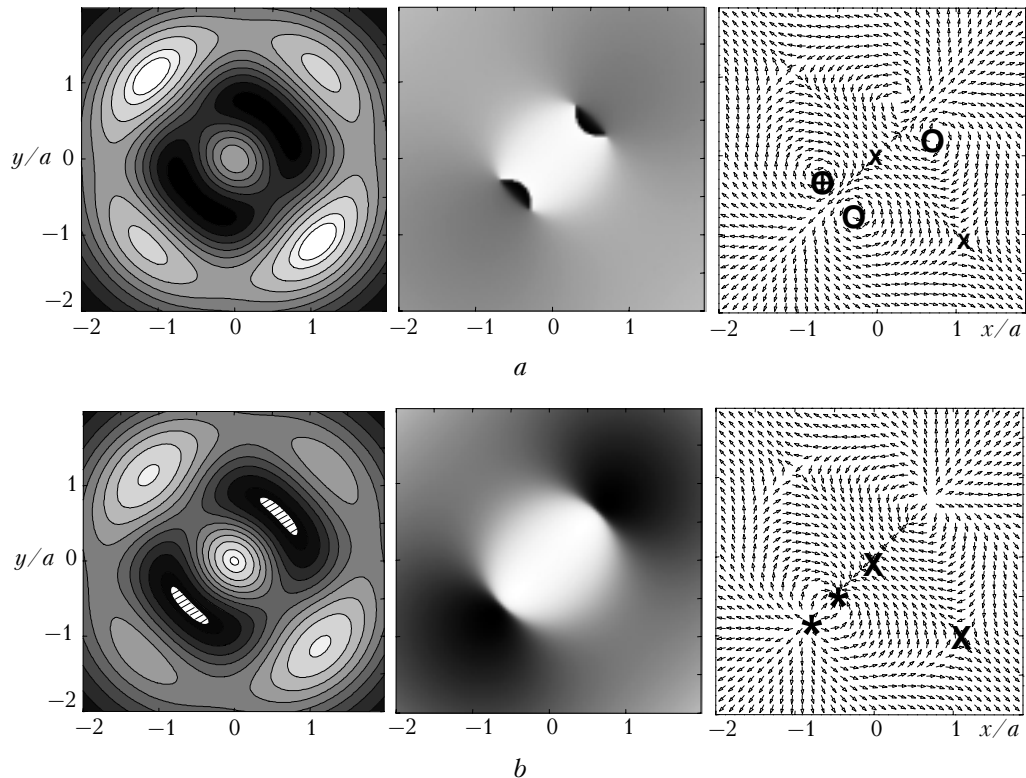


Fig. 1. Distribution of intensity, main phase value, and field of directions in the cross plane in the presence of dislocations $\Omega = 5.0$ (a) and after annihilation of dislocations $\Omega = 2.5$ (b). The positions of singular points are shown as \bigcirc for focus, \bigotimes for node, and \times for saddle. In the first column of Fig. 1b the shaded area corresponds to vortex backwash.

Calculate now the distribution of the complete phase in the plane z_1 using Eq. (21) and the phase distribution in the plane z_0 as the initial one. The necessary stage in calculation of the complete phase is calculation of the lines of energy flow or diffraction rays, which were drawn through numerical solution of Eqs. (22) by the Euler method with automatic step selection. The family of rays going from the plane z_0 spirals around the trajectory of the optical vortex as shown in Fig. 2. This vortex is marked by the sign \oplus in Fig. 1. One can see that after annihilation of optical vortices having opposite signs the spiral trajectory of the rays becomes close to the straight line. It should be noted that in the calculations we controlled fulfillment of condition (16) of applicability of the parabolic approximation and in the calculations of the complete phase we used only the rays for which the condition $|\partial S'/\partial z| \leq 0.1k_0$ holds. In addition, we restricted our consideration to the rays, at which the condition of small angles (23) was fulfilled (they were far from the singular point). So when calculating the complete phase we could use Eq. (25). The absolute error in calculation of the phase change by diffraction rays was 0.01π . Figure 3 depicts the distribution of the complete phase calculated by Eq. (25) for the plane $z_1 = 10000$ m ($\Omega = 2.493$). This distribution corresponds to the two joint families of the lines of energy flow. Each of the rays comprising these families in the process of the spatial beam evolution spirals around the trajectory of the corresponding optical vortex (field zero-line) and after annihilation of these vortices moves translationally to the beam periphery. Note that the values of the complete phase on the rays comprising these two families significantly exceed the phase value in the adjacent areas. Then the phase calculated was used to draw the wave front surface using the condition $S(\mathbf{p}, z) = \text{const}$.

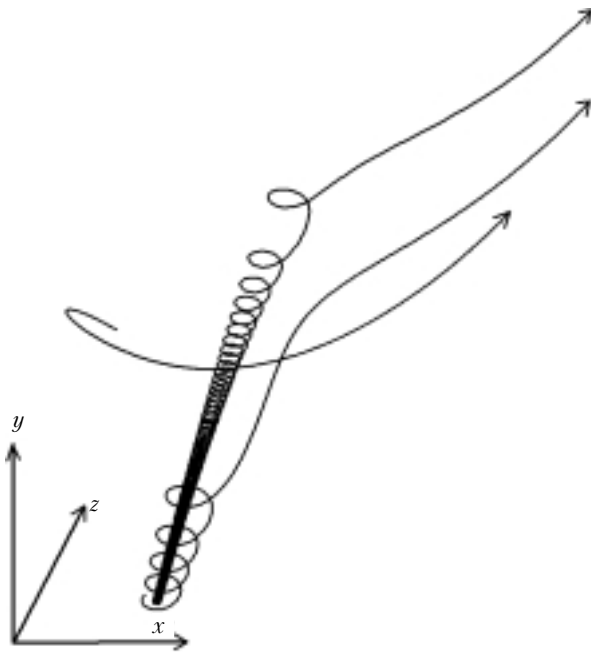


Fig. 2. Diffraction rays near the wave front dislocations.

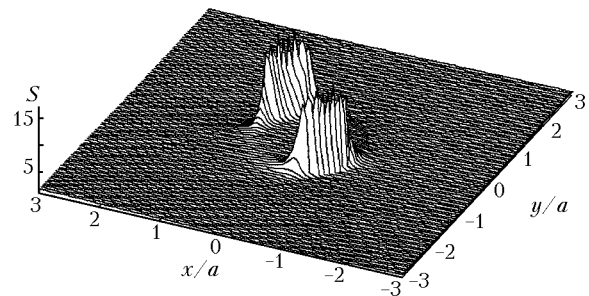


Fig. 3. Phase distribution after annihilation of dislocations. The plot corresponds to the complete phase minus k_0z normalized to π .

The general view of the wave front after annihilation of optical vortices corresponding to the eikonal of 10^4 (the eikonal value is the phase normalized to k_0) is depicted in Fig. 4a. The wave front fragment (Fig. 4b) corresponds to the area bounded by a circle in Fig. 4a. The diffraction rays along which the phase has been calculated are also shown here.

Rays 1, 2 and 3 originate from the points with the coordinates $\{-0.696; -0.365\}$, $\{-0.690; -0.291\}$, $\{-0.691; -0.292\}$, respectively, in the plane $z_0 = 5 \cdot 10^3$ m. The coordinates x and y are normalized to the initial beam radius. Ray 2 is at minimum distance from the vortex center ($\approx 500\lambda$). It follows from Fig. 4a that after annihilation of optical vortices the wave front surface no longer has a helicoid shape. However, it does not become smooth as was believed before, but keeps singularities. These singularities move to the beam periphery with the increasing longitudinal coordinate. If we define the vortex backwash area as the area, in which the complete phase exceeds the total value of the “fast” k_0z and “slow” $\tilde{s}(\mathbf{p}, z)$ phases by more than π radians, then we can find the fraction of energy contained in the vortex backwash areas of the singular field. To do this, it is sufficient to integrate the intensity distribution within the vortex backwash areas (Fig. 1b) and relate the obtained value to the total beam energy P_0 . Since the energy of the vortex backwash areas is formed due to small intensity values near zero-lines, we should expect proportionally small values of the energy contained within these areas. Thus, for the situation shown in Fig. 1b the fraction of energy contained in the vortex backwash areas is only about 2% of the total beam energy. The size of this area turns out to be comparable with the effective scale of the Gaussian in Eq. (26). Note that if we introduce the effective beam size ρ_e as

$$\rho_e^2 = \frac{1}{P_0} \int_{-\infty}^{\infty} I(\mathbf{p}) \rho^2 d^2\rho,$$

then from Eq. (26) we get $\rho_e(z_0)/a = 1.84$ and $\rho_e(z_1)/a = 1.91$.

The vortex backwash area can also be localized using such wave front characteristics as the mean $h(\mathbf{p}, z) = -\Delta_{\perp} S' / (2k_0)$ and Gaussian curvatures¹⁵

$$\rho(\mathbf{p}, z) = \frac{1}{k_0^2} \left[\frac{\partial^2}{\partial x^2} S' \frac{\partial^2}{\partial y^2} S' - \left(\frac{\partial^2}{\partial x \partial y} S' \right)^2 \right],$$

which allow

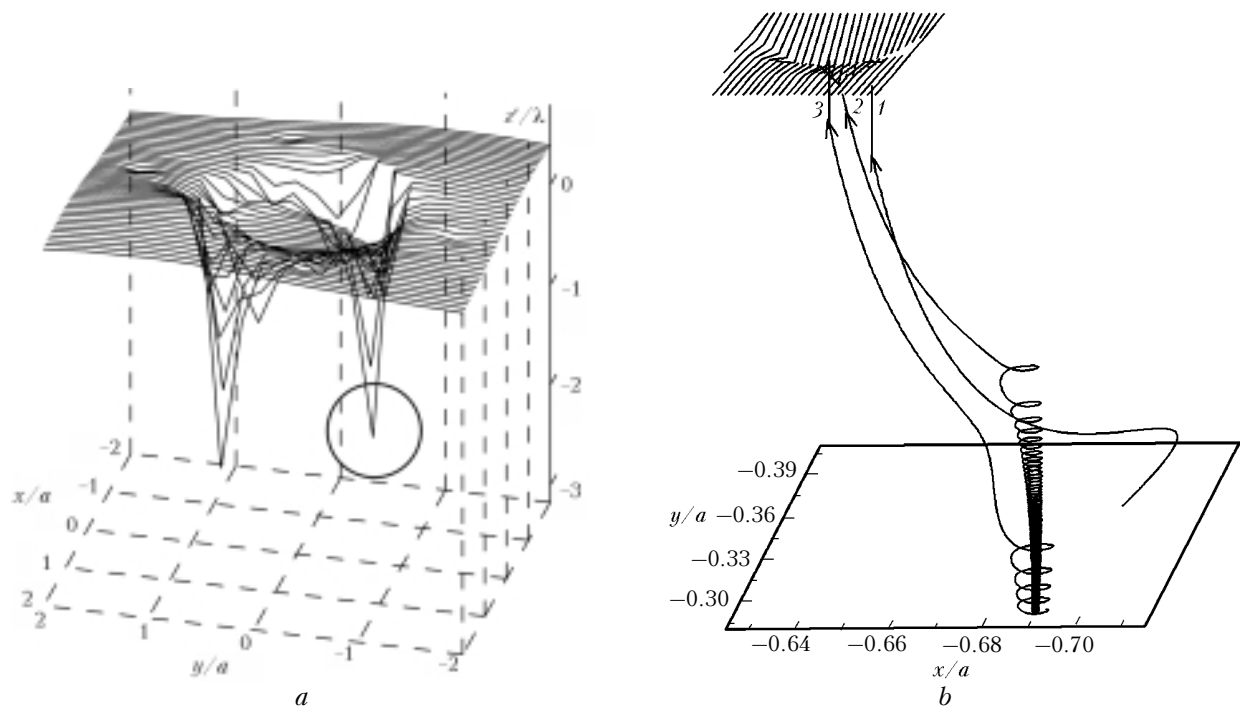


Fig. 4. General view of the beam wave front; $z' = z - z_1$.

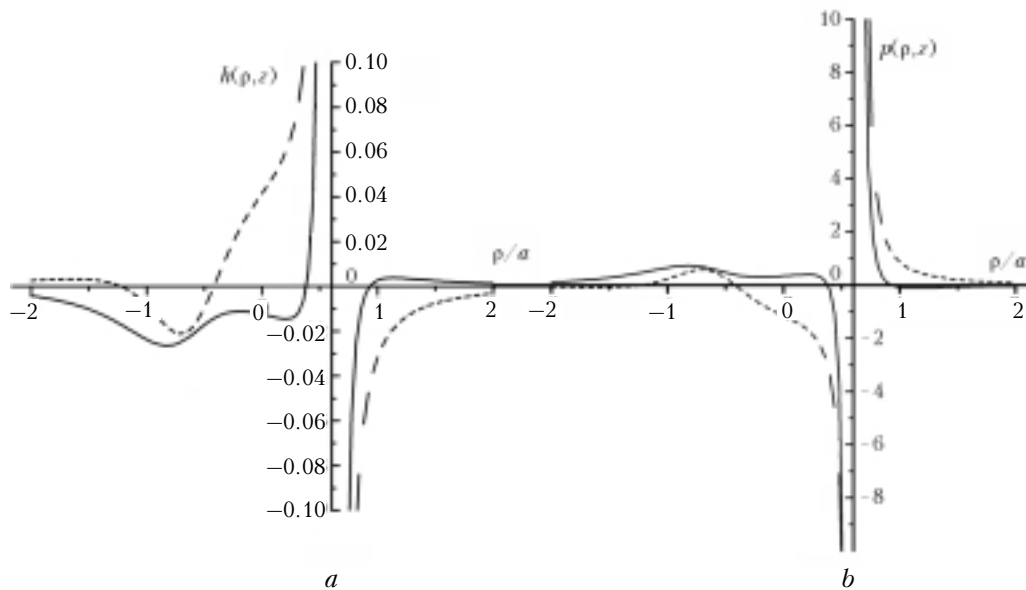


Fig. 5. Distribution of the mean curvature (a) and Gaussian curvature (b) of the phase front in the plane $z_1 = 10^4$ m. Cross sections of these functions by two planes parallel to the coordinate planes xOz (solid line) and yOz (dashed line) intersecting at the center of the vortex backwash area are depicted.

us to evaluate the possibility of locally approximating the wave front by a second-order surface. These functions should obviously be singular in the area of existence of optical vortices, but the calculations show that these functions keep their singular behavior even after annihilation of the vortices. The cross sections of the mean and Gaussian curvatures of the wave front in two mutually normal planes intersecting each other at the center of the vortex backwash area are depicted in Figs. 5a and b, respectively.

It follows from Fig. 5 that as the observation point approaches the center of the vortex backwash area, the wave front curvature increases unlimitedly in the absolute value, which means that the zone of the wave front surface, which can be approximated by a second-order surface, tends to vanish.

Despite our study of the vortex backwash effect has been performed for the simplest field with optical vortices taken as an example, this effect obviously has the general character and it should be taken into

account when dealing with all singular fields, in which vortex annihilation occurs. In particular, this effect should be taken into account in developing principles for construction of single-mirror and many-mirror adaptive optics systems operated based on the phase conjugation method under conditions of strong turbulence.^{16–18} This applies, in particular, to the idea⁶ of using, for phase compensation of screw-type dislocations, of two flexible adaptive mirrors, first for annihilation of optical vortices with the opposite signs and second for reversal of the already smooth wave front.

Conclusion

Thus, using the simplest example of the singular wave field containing optical vortices, we have demonstrated and studied the vortex backwash effect consisting in that the annihilation of optical vortices with the opposite topological charge, which is one of the stages of the vortex life cycle in a singular optical beam, does not lead, as was believed before, to transformation of the singular wave front into the smooth one.

Despite the fact that field zeros and screw wave front dislocations vanish, the wave front near localization of the family of rays taking part in the beam spiral propagation around the field zero-lines still keeps singularities that consist in significantly larger wave front tilts and complete phase in such local areas as compared to the corresponding values of the tilt and phase in the adjacent regions. The absolute values of the mean curvature and Gaussian curvature of wave front parts in the vortex backwash areas increase unlimitedly.

The trail of annihilated optical vortices holds, drifting to the beam periphery in the process of the following propagation. This leads to the need of taking the vortex backwash effect into account in developing adaptive optical systems for compensation for beam distortions under conditions of developed speckle fields, in particular, in the turbulent atmosphere.

References

1. M. Berry, in: *Physics of Defects*, ed. by R. Balian, M. Kleman, and J.-P. Poirier (1981), pp. 453–543.
2. M. Vasnetsov and K. Staliuna, eds., *Optical Vortices. Horizons in World Physics* (Nova Science, New York, 1999), Vol. 228, 218 pp.
3. M.S. Soskin and M.V. Vasnetsov, *Progress in Optics* **42**, 219–276 (2001).
4. A. Primmerman, R. Pries, R.A. Humphreys, B.G. Zollars, H.T. Barclay, and J. Herrmann, *Appl. Opt.* **34**, 2081–2088 (1995).
5. L. Allen, M.J. Padgett, and M. Babiker, *Progress in Optics* **39**, 291–372 (1999).
6. N.B. Baranova and B.Ya. Zel'dovich, *Zh. Eksp. Teor. Fiz.* **80**, No. 5, 1789–1797 (1989).
7. Yu.A. Kravtsov and Yu.I. Orlov, *Geometrical Optics of Inhomogeneous Media* (Nauka, Moscow, 1980), 304 pp.
8. V.I. Bespalov, A.G. Litvak, and V.I. Talanov, in: *Nonlinear Optics. Proc. of the Second Symposium on Nonlinear Optics* (Nauka, Novosibirsk, 1968), pp. 428–463.
9. V.V. Kolosov, *Atmos. Oceanic Opt.* **5**, No. 4, 255–258 (1992).
10. V.P. Aksenov, I.V. Izmailov, B.N. Poizner, and O.V. Tikhomirova, *Opt. Spektrosk.* **92**, No. 3, 465–474 (2002).
11. A.G. Marchuk, in: *Ill-Posed Mathematical Problems of Geophysics*, ed. by M.M. Lavrent'ev and A.S. Alekseev, (CC SB AS USSR, Novosibirsk, 1976), pp. 130–134.
12. D.L. Fried, *J. Opt. Soc. Am. A*, No. 15, 2759–2768 (1998).
13. V.P. Aksenov and O.V. Tikhomirova, *J. Opt. Soc. Am. A* **19**, 345–355 (2002).
14. A.P. Sukhorukov, *Nonlinear Wave Interactions in Optics and Radiophysics* (Nauka, Moscow, 1988), 232 pp.
15. A.N. Malakhov and A.I. Saichev, *Zh. Eksp. Teor. Fiz.* **67**, No. 6(12), 2080–2086 (1974).
16. N.B. Baranova, A.V. Mamaev, N. Pilipeskii, V.V. Skunov, and B.Ya. Zel'dovich, *J. Opt. Soc. Am.* **73**, No. 5, 525–528 (1983).
17. N.V. Vysotina, N.N. Rozanov, V.E. Semenov, and V.A. Smirnov, *Izv. Vyssh. Uchebn. Zaved., Ser. Fiz.*, No. 11, 42–51 (1985).
18. F.Yu. Kanev, V.P. Lukin, and N.A. Makenova, *Atmos. Oceanic Opt.* **15**, No. 12, 973–977 (2002).